

FEDSM-ICNMM2010-30459

THE INFLUENCE OF POLYMERS ON COHERENT STRUCTURES IN DECAYING HOMOGENEOUS ISOTROPIC TURBULENCE

Wei-Hua Cai, Hong-Na Zhang, Feng-Chen Li[†]

School of Energy Science and Engineering, Harbin Institute of Technology, Harbin 150001, China
lifch@hit.edu.cn

ABSTRACT

Drag reduction in decaying homogeneous isotropic turbulence (DHIT) with polymer additives has been observed, which leads to weaker turbulent characteristic quantities. Coherent structures play an important role in the understanding of turbulent dynamics, and the introduction of polymer additives can significantly modify their behavior. It is believed the modifications are closely related to drag reduction mechanism. In the present study, we mainly focus on investigating the influence of polymers on coherent structures from phenomenological and energetic viewpoint for DHIT with polymers based on direct numerical simulation (DNS). The results show that polymers can not only suppress the increase rate of the enstrophy and strain but also their productions, leading to a remarkable inhibition of coherent structures especially at fine scale.

NOMENCLATURE

A	symmetric second-order velocity gradient tensor
C	conformation tensor of polymers
E	turbulent kinetic energy at single wavenumber
k	wavenumber in Fourier space
l	computation domain
P	first invariant of velocity gradient tensor
p	local pressure
Q	second invariant of velocity gradient tensor
r^2	extension length of polymer molecule
R	third invariant of velocity gradient tensor
Re	Reynolds number
S	rate-of-strain tensor
\mathcal{S}	total strain
T	stress tensor
u	velocity vector

W rate-of-rotation tensor

Wi Weissenberg number

Greek Letters

Δ	discriminant of velocity gradient tensor
Ω	enstrophy
β	measure of polymer solution concentration
ε	turbulent energy dissipation rate
λ	the eigenvalue of velocity gradient tensor
ν	kinematic viscosity
ξ	total turbulent kinetic energy
ρ	solvent density
τ	relaxation time of polymers
ω	vorticity vector

Subscript

i,j,k	index of Cartesian coordinate
p	index of polymer solution
m	instant time when the decaying rate of turbulent kinetic energy reaches the maximum value
λ	Taylor microscale
$+$	index of the largest remaining eigenvalue
$-$	index of the smallest remaining eigenvalue
th	index of the positive threshold
z	index of the eigenvalues associated with eigenvector that is maximally aligned with velocity vector

Superscript

N	index of Newtonian fluid
p	index of polymer solution
s	index of solvent
T	transposition of the vector

INTRODUCTION

Turbulent drag reduction (DR) by additives is an intriguing phenomenon discovered by Toms [1], which shows that adding a small concentration of polymer or some kind of surfactant

[†] Corresponding author

additives may cause a dramatic frictional DR. Since then numerous attention has been paid to figure out the turbulent characteristics and DR mechanism with additives [2][3][4][5]. To interpret DR phenomenon two famous theories have been proposed. Lumley [2] proposed the viscous theory (i.e. ‘time criterion’ approach), in which he emphasized highly the major role of wall. However, some grid-turbulence experiments of dilute polymer solutions have shown that DR can occur without the presence of wall (or far from the wall) [6][7][8]. Then Tabor and de Gennes [9][10] proposed an elastic theory based on homogeneous isotropic turbulence, which neglects the viscous effect in Lumley’s theory. This theory has received some supports in recent experiments [11][12] and numerical simulations for homogenous isotropic turbulence [13][14]. These studies showed that with the presence of polymers there exists remarkable inhibition effects of vortical structures, a reduction of turbulent energy dissipation and a significant modification of the classical Kolmogorov energy cascade in HIT without wall effect. But, since the problem is actually a combination of two most complicated and poorly understood problems, turbulence and polymer solution dynamics, in spite of enormous efforts from different aspects, the physical DR mechanism is still poorly understood and needs further research.

As is known, there exist coherent and ordered structures in turbulent flow since the direct observation of these structures in turbulent shear layer by Kline [15]. They can be roughly divided into two groups: those with tubular or filamentary structures (vortex tubes) and those with nonfilamentary vorticity distributions (vortex sheets). Researches show that vortex tubes play an important role in the overall turbulence dynamics such as vortex ‘worms’ or ‘filament’ in isotropic turbulence [16][17][18], quasi-streamwise vortices [19] and ‘hairpin’ vortices in wall turbulence [20]. The formation of vortex tubes is often attributed to rolling-up of the vortex sheets due to the Kelvin-Helmholtz instability. As for the sheet-like structures the most prominent characteristic feature is that in the region the strain rate and vorticity are highly correlated, their magnitudes are comparably equal, and considerable dissipation of turbulent kinetic energy which is final result of energy cascade takes place [21]. The existence of coherent structures is one of the most important characteristics in turbulence. And in polymer solution flow the introduction of polymer additives can significantly modify the behavior and properties of coherent structures. We believe the modifications are closely related to DR mechanism. So in this paper, we mainly focus on investigating the influence of polymers on vortex tubes and sheets from phenomenological and energetic viewpoint for decaying homogeneous isotropic turbulence (DHIT) with polymer additives based on direct numerical simulation (DNS).

The paper is organized as follows. In section II and III the numerical method for DNS and vortex-identification methods used in the paper are introduced. In section IV the results and discussion based on the enstrophy and strain analysis and the

visualization of vortex structures at different scales are presented. Section V gives the conclusions of our study.

NUMERICAL SIMULATION

We carried out DNS for incompressible fluid with and without polymer additives based on Navier-Stokes (N-S) equation coupled with the finitely extensible nonlinear elastic Peterlin (FENE-P) model.

The governing equations for DHIT of dilute polymer solutions are as follows:

$$\partial \mathbf{u} / \partial t + \mathbf{u} \cdot \nabla \mathbf{u} = -\nabla p / \rho + \nabla \cdot \mathbf{T}^{[s]} / \rho + \nabla \cdot \mathbf{T}^{[p]} / \rho, \quad (1)$$

$$\partial \mathbf{C} / \partial t + \mathbf{u} \cdot \nabla \mathbf{C} = \mathbf{C} \cdot \nabla \mathbf{u} + \nabla \mathbf{u}^T \cdot \mathbf{C} - (f(r)\mathbf{C} - \mathbf{I}) / \tau_p, \quad (2)$$

where $\mathbf{u}(\mathbf{x}, t)$ is the velocity vector; $p(\mathbf{x}, t)$ the local pressure; ρ the fluid density; $\mathbf{T}^{[s]} = 2\rho\nu^{[s]}\mathbf{S}$ the Newtonian stress due to the solvent, $\nu^{[s]}$ the solvent kinematic viscosity and $\mathbf{S} = (\nabla \mathbf{u} + \nabla \mathbf{u}^T) / 2$ the rate of strain tensor the rate of strain tensor; $\mathbf{T}^{[p]} = \rho\nu^{[p]}(f(r)\mathbf{C} - \mathbf{I}) / \tau_p$ the polymer stress, $\nu^{[p]}$ the polymer kinematic viscosity, τ_p the polymer relaxation time, \mathbf{C}_{ij} the conformation tensor. In the FENE-P model, $f(r) = (L^2 - 3) / (L^2 - r^2)$ ensures the finite extensibility; $r^2 = \text{trace}(\mathbf{C})$ and L are the extension length and the maximum possible extension of polymer, respectively.

To solve Eq.(1), a standard pseudo-spectral code with 96^3 collocation points in the periodic cubic domain of size $l = 2\pi$ is used for spatial discretization [22][23] with all the nonlinear terms fully de-aliased by the 3/2 rule. Note that in the simulations the spatial resolution is sufficient to capture the information at the smallest scale (i.e., Kolmogorov scale). A second-order Adams-Bashforth scheme is adopted for time advancement. To solve Eq.(2), for spatial discretization a second-order central difference scheme are used except for convective term using the second-order Kurganov-Tadmor (KT) scheme [24] and for time marching a second-order Adams-Bashforth scheme is adopted.

The initial velocity field is obtained based on Rogallo’s procedure [22] and the initial energy spectra $E_0(k) = 0.01k^4 \exp(-0.14k^2)$. For initial conformation field, polymers were assumed non-stretched, corresponding to $C_{ij}^0(x, y, z) = \delta_{ij}$ [25][26]. In Fourier space, the turbulent kinetic energy spectra $E(k, t) = \sum_{k-1/2 < k' \leq k+1/2} |\mathbf{u}_{k'}(t)|^2 / 2$, the total kinetic energy $\xi(t) = \sum_k E(k, t)$, and in physical space $\xi(t) = \int_{\beta} u_i^2(\mathbf{x}, t) / 2 dV$; the energy-dissipation rate in Fourier space $\varepsilon(t) = \nu^{[s]} \sum_k k^2 E(k, t)$, and in physical space $\varepsilon(t) = \int_{\beta} \nu^{[s]} S_{ij}^2 dV$. The Taylor-microscale is defined as $\lambda = \sqrt{15\nu^{[s]} \langle u^2 \rangle / \varepsilon(t)}$, where $\langle u^2 \rangle = 2\xi(t) / 3$ is turbulent fluctuation intensity. The Taylor-microscale Reynolds number Re_λ and the Weissenberg number Wi are defined as

$Re_\lambda = \sqrt{20} \xi^{N,m} / \sqrt{3 v^{[s]} \varepsilon^{N,m}}$ and $Wi = \tau_p \sqrt{\varepsilon^{N,m} / v^{[s]}}$, respectively, where the energy-dissipation rate $\varepsilon^{N,m}$ is chosen at $t = t_m$ in Fourier space; here, t_m corresponds to the moment at which ε reaches to its maximum amplitude; the superscript “N” represents the Newtonian fluid case. In this paper, the basic parameters are as following: $Re_\lambda = 26.2$, $Wi = 0.62$, $\tau_p = 0.1$ s, $\beta = 0.6$ (a dimensionless measure of dilute polymer solution concentration, and smaller β corresponds to denser polymer solution) for polymer solution case and $Re_\lambda = 26.2$ for Newtonian fluid case.

VORTEX-IDENTIFYING METHODS

To identify vortex tubes, several local methods have been considered based on the second invariant (Q), discriminant (Δ) or eigenvalues (λ_2, λ_{ci}) of velocity gradient tensor ($\nabla \mathbf{u}$) [27][28][29][30]. In our paper, we use the invariant Q method to identify vortex tubes.

In turbulent flow studies, velocity derivatives play an important role studying exploring turbulent dynamics. The velocity-gradient tensor can be split into symmetric and anti-symmetric parts [27][30]:

$$\nabla \mathbf{u} = S_{ij} + W_{ij}, \quad (3)$$

where $S_{ij} = (\partial u_i / \partial x_j + \partial u_j / \partial x_i) / 2$ the rate-of-strain tensor and $W_{ij} = (\partial u_i / \partial x_j - \partial u_j / \partial x_i) / 2$ the rate-of-rotation tensor. The eigenvalues of $\partial u_i / \partial x_j$ satisfy the characteristic equation:

$$\lambda^3 + P\lambda^2 + Q\lambda + R = 0, \quad (4)$$

where the three invariants are

$$P = S_{ii}, \quad Q = (P^2 - S_{ij}S_{ji} - W_{ij}W_{ji}) / 2, \quad (5), (6)$$

$$R = (-P^3 + 3PQ - S_{ij}S_{jk}S_{ki} - 3W_{ij}W_{jk}W_{ki}) / 3.$$

And for incompressible flow,

$$P = 0, \quad Q = (W_{ij}W_{ij} - S_{ij}S_{ij}) / 2,$$

$$R = (-S_{ij}S_{jk}S_{ki} - 3W_{ij}W_{jk}W_{ki}) / 3. \quad (7)$$

The second invariant Q reflects the relative strength of rate of rotation and rate of strain. The first term of Q is proportional to the enstrophy density and the second term is proportional to the dissipation rate of kinetic energy. The positive Q isosurfaces isolate the areas where the strength of the rotation are larger than that of the strain, thus an tubelike zone can be defined as a region with the positive Q isosurfaces [287][30]. Additionally, the pressure in the eddy region is required to be lower than the ambient pressure. Though $Q > 0$ does not guarantee the existence of a pressure minimum inside the region identified by it [29], in most cases the pressure condition is satisfied.

However, unlike vortex tubes very few identification methods [31][32] for vortex sheet-like structures have been proposed because the vortex sheets are more disorganized than

the vortex tubes and susceptible to small disturbances, which makes it fairly difficult to be examined in turbulent flows. Recently Horiuti and Takagi [21] proposed a new definition based on the eigendecomposition of the symmetric second-order velocity gradient tensor, $A_{ij} = S_{ik}W_{kj} + S_{jk}W_{ki}$. Since $A_{ii} = 0$, the eigenvalues of A_{ij} are obtained from the equation:

$$x^3 - (A_{ij}A_{ji})x / 2 - A_{ij}A_{jk}A_{ki} / 3 = 0. \quad (8)$$

Then, denoting $[A_{ij}]_z$, $[A_{ij}]_+$, and $[A_{ij}]_-$ as the eigenvalues associated with the eigenvector that is maximally aligned with the velocity vector, the largest remaining and the smallest eigenvalue, respectively. It is observed that vortex sheets can be examined based on the criterion:

$$[A_{ij}]_+ > \{[A_{ij}]_+\}_{th}, \quad (9)$$

where $\{[A_{ij}]_+\}_{th}$ is an arbitrary positive threshold.

RESULTS AND DISCUSSION

The enstrophy indicates the strength of vortex structures and mainly generated by the stretching of vortex tubes which is regarded as the impetus of turbulence maintenance. Tennekes and Lumley [33] argued that vortex stretching is the physical mechanism leading to the hypothesized energy cascade from large to fine scales. However, energy dissipation (the final results of energy cascade) is directly associated with total strain. Tsinober [34] noted that in physical space the production of strain or dissipation is not exactly due to vortex stretching but due to vortex compression. He also emphasized the importance of strain as the vorticity in the context of creation and maintenance of turbulence. Anyway it is necessary to study the properties of both strain and vorticity to explore turbulence nature. So to figure out how the polymer additives act on turbulent vortex structures in DHIT, we firstly research the alterations and productions of the enstrophy and strain, respectively, after adding polymer additives. Then the visualizations of vortex tubes and sheets at different scales in DHIT for both Newtonian fluid and polymer solution cases are shown to give an intuitive understanding.

Enstrophy analysis

Based on Eq.(1), it is easy to deduce the enstrophy transport equation of DHIT for polymer solution case, as follows [14]:

$$\underbrace{\frac{\partial \langle \Omega \rangle}{\partial t}}_{\text{enstrophy increase rate}} = \underbrace{\langle \omega_i S_{ij} \omega_j \rangle}_{\text{enstrophy production}} + \underbrace{v^{[s]} \langle \omega_i \frac{\partial^2 \omega_i}{\partial x_j \partial x_j} \rangle}_{\text{enstrophy dissipation}}, \quad (10)$$

$$+ \underbrace{\langle \omega_i \frac{\partial^2 T_{mj}^{[p]}}{\partial x_m \partial x_n} \varepsilon_{nji} \rangle}_{\text{polymers effect}}$$

where the operator $\langle \cdot \rangle$ denotes ensemble average; ε_{nji} the permutation symbol; ω_i the i th component of the vorticity $\boldsymbol{\omega} = \nabla \times \mathbf{u}$; and $\Omega = \omega_i \omega_i / 2$ the enstrophy; $S_{ens} = \omega_i S_{ij} \omega_j$ the enstrophy production, which is due to the interaction

between vorticity and strain; $V_{ens} = \nu^{[s]} \omega_i \frac{\partial^2 \omega_i}{\partial x_j \partial x_j}$ the enstrophy

dissipation; and $P_{ens} = \omega_i \frac{\partial^2 T_{ij}^{[p]}}{\partial x_m \partial x_n} \epsilon_{nji}$ the polymers effect, which

is due to interaction between vorticity and polymers elastic stress (or polymer conformation) and does not appear in Newtonian fluid case.

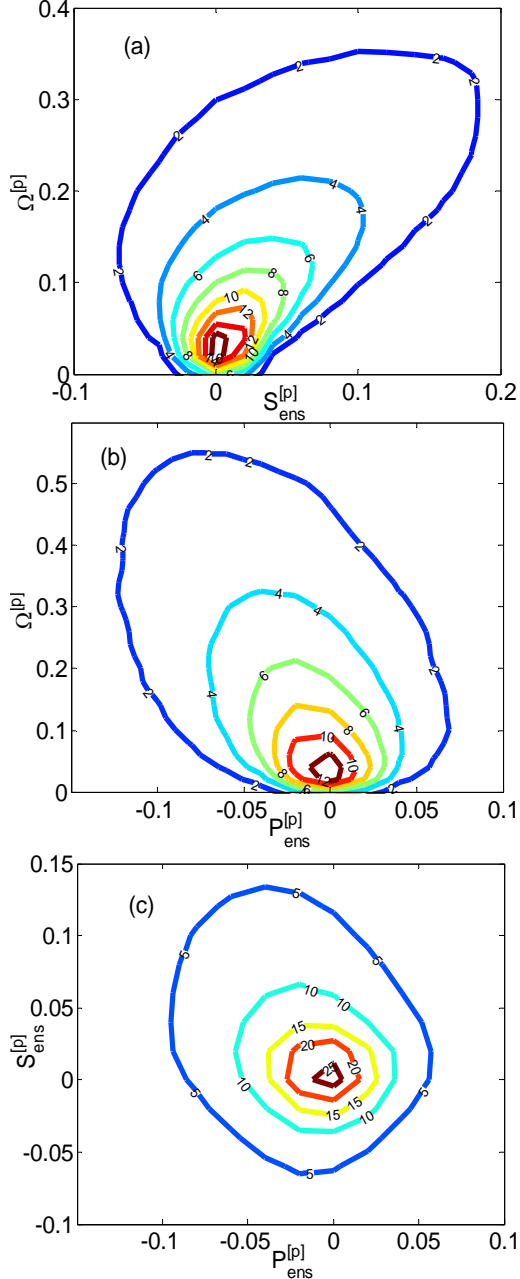


Fig.1. JPDF at $t=0.6s$ for polymer solution case ($Wi=0.62$, $\beta=0.6$). (a) $S_{ens}^{[p]}$ vs. $\Omega^{[p]}$; (b) $P_{ens}^{[p]}$ vs. $\Omega^{[p]}$; (c) $P_{ens}^{[p]}$ vs. $S_{ens}^{[p]}$.

Firstly joint probability density function (JPDF) of the enstrophy production $S_{ens}^{[p]}$ versus the enstrophy $\Omega^{[p]}$ for polymer solution case at $t=0.6s$ (the enstrophy reaches the maximum value at this time) is shown in Fig.1(a), from which a strong positive correlation can be observed. It confirms the contribution of vortex stretching ($S_{ens}^{[p]} > 0$) to the enstrophy $\Omega^{[p]}$. And to interpret the influence of polymers $P_{ens}^{[p]}$ on the enstrophy $\Omega^{[p]}$ and its production $S_{ens}^{[p]}$, their JPDFs are shown in Figs.1(b) and 1(c). It can be clearly seen that the polymer effect $P_{ens}^{[p]}$ is also strongly correlated with the enstrophy $\Omega^{[p]}$ and its production $S_{ens}^{[p]}$. The polymer effect $P_{ens}^{[p]}$ is negatively skewed, which suggests that the polymers conformation counters to the rotation of flow structures so as to increase the “vortex stretching resistance” of flow structures. It also has a similar order of magnitude to that of the enstrophy production, indicating a strong baffling feedback on flow structures because of its elastic nature, which can almost counteract the effects of vortex stretching. Finally due to the elastic nature the enstrophy (strength of vorticity) and its production (a source of turbulence maintenance) are undoubtedly reduced with the presence of polymers as compared with that of Newtonian fluid case to produce the DR phenomenon. From the phenomenological viewpoint, the introduction of polymer additives inhibits the generation of tubes, where the vorticity dominated. The results can be validated by the visualization of vortex tubes at different scales (as shown in Fig.4).

Strain analysis

We also deduced the mean strain transport equation of DHIT with polymer additives [14]:

$$\frac{\partial \langle \mathbb{S} \rangle}{\partial t} = \underbrace{-\langle S_{ik} S_{kj} S_{ij} \rangle}_{\text{strain production}} - \underbrace{\frac{1}{4} \langle \omega_i \omega_j S_{ij} \rangle}_{\text{vortex stretching effect}} + \underbrace{\nu^{[s]} \langle S_{ij} \nabla^2 S_{ij} \rangle}_{\text{strain viscous dissipation}} + \underbrace{\langle \frac{\partial^2 T_{ik}^{[p]}}{\partial x_k \partial x_j} S_{ij} \rangle}_{\text{polymers effect}}, \quad (11)$$

where $\mathbb{S} = S_{ij} S_{ij} / 2$ the total strain; $S_{str} = -S_{ik} S_{kj} S_{ij}$ the strain production which is from strain self-amplification; $W_{str} = \omega_i \omega_j S_{ij} / 4$ the enstrophy production effect on the total strain; $V_{str} = \nu^{[s]} S_{ij} \nabla^2 S_{ij}$ the strain viscous dissipation;

$P_{str} = \frac{\partial^2 T_{ik}^{[p]}}{\partial x_k \partial x_j} S_{ij}$ the polymers effect which is due to the interaction between strain and polymers elastic stress (or polymers conformation) and does not appear in Newtonian fluid case.

Similarly we study the JPDF at $t=0.6s$ for the corresponding term of Eq.(9) in order to expatiate the effect of polymer additives on the strain, as shown in Fig.2. The JPDF of the strain production $S_{str}^{[p]}$ versus the strain $S_{ij}^{[p]} S_{ij}^{[p]} / 2$ in Fig.2(a) shows a strong positive correlation indicating that the main source of the strain is from its self-amplification. And the

JPDFs of the polymers effect $P_{str}^{[p]}$ on the total strain $S_{ij}^{[p]}S_{ij}^{[p]}/2$ and its production $S_{str}^{[p]}$ are shown in Fig.2(b) and 2(c), respectively. As expected, the polymers effect $P_{str}^{[p]}$ is negatively skewed, which means the polymers conformation mostly counters to the strain of flow structures so as to increase the “strain generation resistance” of flow structures. Besides, we observed that the polymers effect $P_{str}^{[p]}$ has a similar order of magnitude to that of the strain production $S_{str}^{[p]}$, indicating that the effects are pronounced and can counteract the strain self-amplification to some extent. In this way the strain in the polymer solution case can be suppressed, then the strain self-amplification reduced and so on. From the phenomenological viewpoint, the introduction of polymer additives inhibits the generation of vortex sheet-like structures, where the strain dominated and most energy dissipation occurs. The results are validated by the visualization of vortex sheet-like structures at different scales (as shown in Fig. 5).

Coherent structure visualization

In this part we visualize the vortex tubes and sheets at different scales for DHIT with and without polymer additives based on Q method [27][30] and Horiuti & Takagi method [21] respectively, shown in Figs.4 and 5. Usually the choice of the threshold value changes the appearance of the flow field, for instance, raising the threshold value too high will result in losing some important vortices and setting the threshold value too low will cause an unclear visualization. The threshold value is chosen so that a large number of vortices could be visualized and at the same time different vortices could be distinguishable [35]. In the present paper, the isosurface of Q with a threshold $Q_{th} = 2Q'_{rms}$, where Q'_{rms} is the average root mean square of the Q fluctuation [37]. However, it is found that applying the above vortex-identifying method to the whole flow field, the results have a tendency to show only the fine-scale vortical structures. So, the characteristics of the large-scale and intermediate-scale coherent eddy structures will be difficult to study. In order to research the influence of polymers on coherent structures of these scales, low-pass filtering by Fourier transformation is carried out against the flow field shown in Fig.3. First, the velocity field is transformed into Fourier space by FFT, then the high frequency component are removed at three different thresholds and finally returned to physical space [35]. The velocity field at $t=2s$ (i.e. the time in the energy decaying period) is filtered in Fourier space by different cut-off frequencies:

$$u(x) = \sum_{|k| \leq k_c} \hat{u}(k) e^{ikx}, \quad (11)$$

where all modes greater than the cut-off wavenumber k_c are set to zero. In our study, the flow field is divided into three parts of different scales: large-scale ($0 < k \leq 4$), intermediate-scale ($0 < k \leq 8$) and fine-scale (the whole field). The energy spectrum is calculated for each scale using the same energy spectrum function.

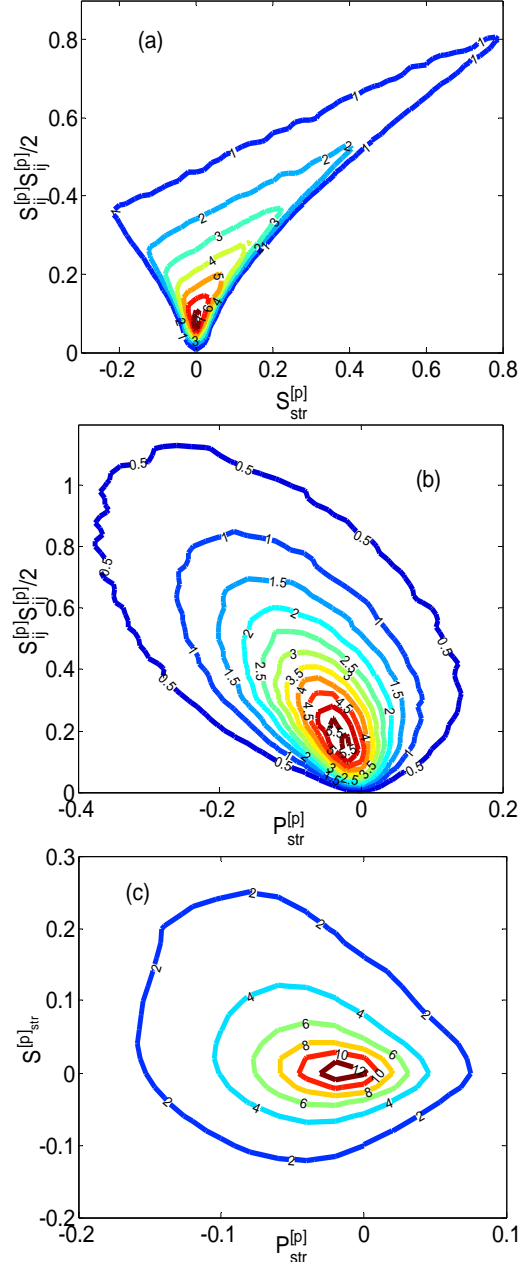


Fig.2. JPDF at $t=0.6s$ for polymer solution case ($Wi=0.62$, $\beta=0.6$). (a) $S_{str}^{[p]}$ vs. $S_{ij}^{[p]}S_{ij}^{[p]}/2$; (b) $P_{str}^{[p]}$ vs. $S_{ij}^{[p]}S_{ij}^{[p]}/2$; (c) $P_{str}^{[p]}$ vs. $S_{str}^{[p]}$.

From Figs.4 and 5, a remarkable decrease of intermediate-scale and fine-scale vortex tubes and sheets can be observed in DHIT with polymer additives as compared to Newtonian fluid case. However, at large-scale, the inhibition effect by polymer additives is not as distinct as that at other scales. Based on the above analyses of the enstrophy and the strain, this is not surprising. It is relevant to the negative influence of polymer additives on the enstrophy and the strain production which can be regarded as the impetus of fine-scale vortex tubes and

sheets. And from micro-perspective, it shows that polymer additives can directly act on the structures at fine-scale and even terminate subsequent energy cascade to modify the turbulent feature for polymer solution case.

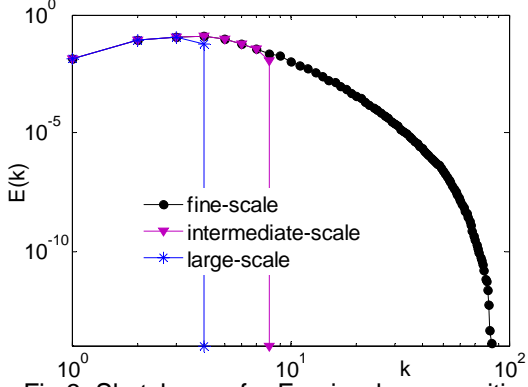


Fig.3. Sketch map for Fourier decomposition

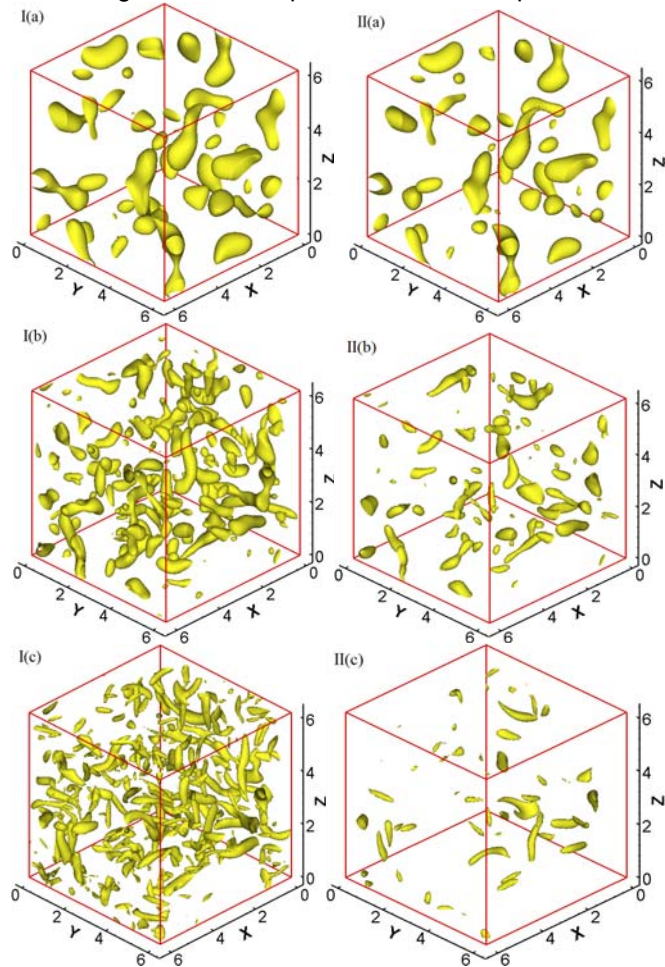


Fig.4. Constant Q isosurface for (I) Newtonian fluid case and (II) polymer solution case in three different scales field at $t=2.0s$. (a) large-scale field ($Q=0.9141$); (b) intermediate-scale field ($Q=4.6695$); (c) fine-scale field ($Q=9.4685$).

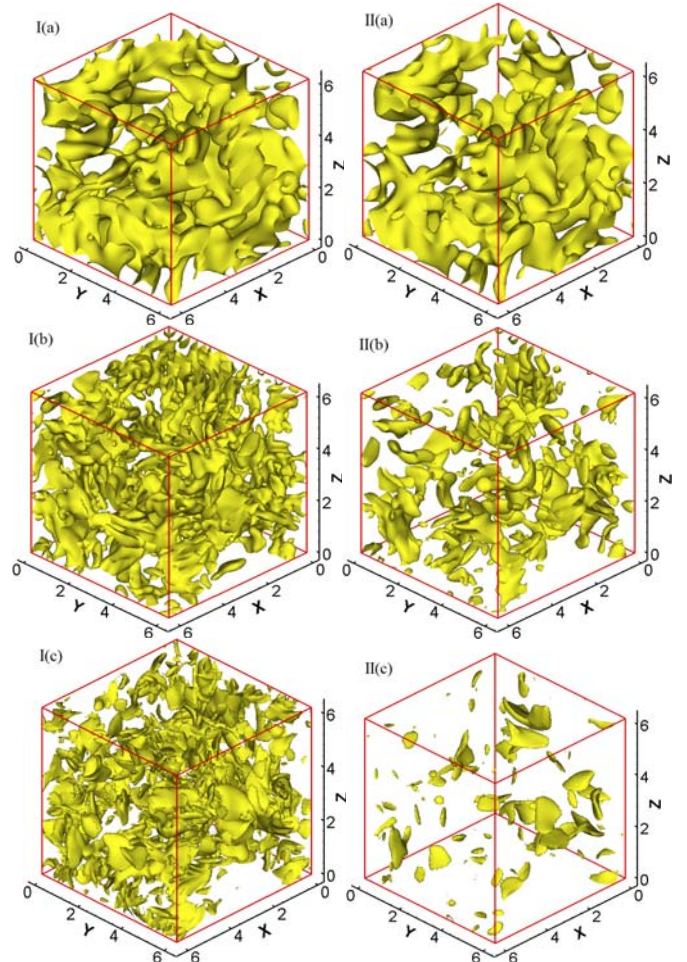


Fig. 5. Constant $[A_{ij}]_+$ isosurface for (I) Newtonian fluid case and (II) polymer solution case in three different scale field at $t=2.0s$. (a) large-scale field ($[A_{ij}]_+=0.6682$); (b) intermediate-scale field ($[A_{ij}]_+=3.6454$); (c) fine-scale field ($[A_{ij}]_+=11.2406$).

CONCLUSIONS

According to the above analysis, we obtain the following conclusions. From the viewpoint of JPDF between the correlation terms in Eqs.(8) and (9), it is obtained that polymer effects are strongly correlated with them. The polymers elastic conformation mostly opposes to the rotation and strain of coherent structures with a pronounced magnitude so as to suppress the increase rate and productions of the enstrophy and strain, respectively. The results are confirmed by the visualizations of vortex tubes and sheets, which show a remarkable inhibition of intermediate-scale and fine-scale vortex structures. From micro-perspective, polymer additives can directly act on the structures at fine-scale, causing important modifications of turbulent nature as compared with

that of Newtonian fluid case. And the modifications refer to weaken turbulent characteristic, which leads to DR effect.

ACKNOWLEDGMENTS

We thank B. Yu and Y. Yamamoto for their discussions on DNS. This study was supported by National Natural Science Foundation of China (Grant No.10872060) and Program for New Century Excellent Talents in University of China (Grant No. NCET-07-0235). The authors are very grateful to the enthusiastic help of all members of Complex Flow and Heat Transfer Laboratory of Harbin Institute of Technology.

REFERENCES

- [1] Toms, B. A., 1949, "Some observation on the flow of linear polymer solutions through straight tubes at large Reynolds number," In Proceedings of the First International Congress of Rheology, North Holland, Amsterdam, **2**, pp. 135-141.
- [2] Lumley, J. L., 1973, "Drag reduction in turbulent flow by polymer additives," *J. Polymer Sci. Macrom. Rew.*, **7**, pp.263-290.
- [3] Sreenivasan, K. R. and White, C. M., 2000, "The onset of drag reduction by dilute polymer additives, and the maximum drag reduction asymptote," *J. Fluid Mech.*, **409**, pp. 149-164.
- [4] Ptasinski, P. K., Nieuwstadt, F. T. M., Hulsen, M. A., Van Den Brule, B. H. A. A., Boersma, B. J. and Hunt, J. C. R., 2003, "Turbulent channel flow near maximum drag reduction: simulations, experiments and mechanisms," *J. Fluid Mech.*, **490**, pp. 251-291
- [5] Li, F.-C., Kawaguchi, Y. and Hishida, K., 2004, "Investigation on the characteristics of turbulence transport for momentum and heat in a drag-reducing surfactant solution flow," *Phys. Fluids*, **16**, pp. 3281-3295.
- [6] Barnard, B. J. S. and Sellin, R. H. J., 1969, "Grid Turbulence in dilute polymer solutions," *Nature, Lond*, **222**, pp. 1160-1162.
- [7] Friehe, C. A. and Schwarz, W. H., 1970, "Grid-generated turbulence in dilute polymer solutions," *J. Fluid Mech.*, **1970**, **44**, pp. 173-193.
- [8] McComb, W. D., Allan, J. and Greated C. A., 1977, "Effect of Polymer Additives on The Small-scale Structure of Grid-generated Turbulence," *Phys. Fluids*, **20**, pp. 873-879.
- [9] de Gennes, P. G., 1986, "Towards a cascade theory of drag reduction," *Physica A*, **140**, pp. 9-25.
- [10] Tabor, M. and de Gennes, P. G., 1986, "A cascade theory of drag reduction," *Europhys. Lett.*, **2**, pp. 519-522.
- [11] van Doorn, E., White, C. M. and Sreenivasan, K. R., 1999, "The decay of grid turbulence in polymer and surfactant solutions," *Phys. Fluids*, **8**, pp. 2387-2393.
- [12] Liberzon, A., Guala, M., Kinzelbach, W. and Tsinober, A., 2006, "On turbulent kinetic energy production and dissipation in dilute polymer solutions," *Phys. Fluids*, **18**(125101), pp. 1-12.
- [13] Jin, S., 2007, "Numerical simulations of a dilute polymer solution in isotropic turbulence," PhD thesis, The Cornell University.
- [14] Cai, W. H., Li, F. C. and Zhang, H. N., 2010, "DNS study of decaying homogeneous isotropic turbulence with polymer additives," *J. Fluid Mech.* (submitted)
- [15] Kline, S. J., Reynolds, W. C., Schraub, F. A. and Runstadler, P. W., 1967, "The structure of turbulent shear layers," *J. Fluid Mech.*, **30**, pp. 741-773.
- [16] Siggia, E. D., 1981, "Numerical study of small scale intermittency in three-dimensional turbulence," *J. Fluid Mech.*, **107**, pp. 375-406.
- [17] Douady, S., Couder, Y. and Brachet, M. E., 1991, "Direct observation of the intermittency of intense vorticity filaments in turbulence," *Phys. Rev. Lett.*, **67**, pp. 983-986.
- [18] Jimenez, J., Wray, A. A., Saffman, P. G., Rogallo, R. S., 1993, "The structure of intense vorticity in homogeneous isotropic turbulence," *J. Fluid Mech.*, **255**, pp. 65-90.
- [19] Robinson, S. K., 1991, "Coherent motion in the turbulent boundary layer," *Annu. Rev. Fluid Mech.*, **23**, pp. 601-639.
- [20] Adrian, R. J., Meinhart, C. D. and Tomkins, C. D., 2000, "Vortex organization in the outer region of the turbulent boundary layer," *J. Fluid Mech.*, **422**, pp. 1-54.
- [21] Horiuti, K. and Takagi, Y., 2005, "Identification method for vortex sheet structures in turbulent flows," *Phys. Fluids*, **17**(121703), pp. 1-4.
- [22] Rogallo, R. S., 1981, "Numerical experiments in homogeneous isotropic turbulence," Technical Report No.81315, NASA.
- [23] Canuto, C., Hussaini, M. Y., Quarteroni, A. and Zang, T. A., 1988, "Spectral methods in fluid dynamics," Springer-Verlag, New York.
- [24] Vaithianathan, T., Robert, A., Bresseur, J. G. and Collins, L. R., 2006, "An improved algorithm for simulating three-dimensional, viscoelastic turbulence," *J. Non-Newtonian Fluid Mech.*, **140**, pp. 3-22.
- [25] Vaithianathan, T., Collins, L. R., 2003, "Numerical approach to simulating turbulent flow of a viscoelastic polymer solution," *J. Compt. Phys.*, **187**, pp. 1-23.
- [26] Perlekar, P., Mitra, D. and Pandit, R., 2006, "Manifestations of drag reduction by polymer additives in decaying, homogenous, isotropic turbulence," *Phy. Rev. Letts.*, **97**(264501), pp. 1-4.
- [27] Hunt, J. C. R., Wray, A. A. and Moin, P., 1988, "Eddies, streams and convergence zones in turbulent flows," Report CTR-S88, Center for Turbulence Research, pp. 193-208.
- [28] Perry, A. E. and Chong, M. S., 1987, "A description of edding motions and flow patterns using critical-point concepts," *Annu. Rev. Fluid Mech.*, **19**, pp. 125-155.
- [29] Jeong, J. and Hussain, F., 1995, "On the definition of a vortex," *J. Fluid Mech.*, **285**, pp. 69-94.
- [30] Zhou, J., Adrian, R. J., Balachandar, S. and Kendall, T. M., 1999, "Mechanisms for generating coherent packets of hairpin vortices in channel flow," *J. Fluid Mech.*, **387**, pp. 353-396.

- [31] Tanaka, M. and Kida, S., 1993, "Characterization of vortex tubes and sheets," *Phys. Fluids*, **5**, pp. 2079-2082.
- [32] Horiuti, K. and Takagi, Y., 2001, "A classification method for vortex sheet and tube structures in turbulent flows. *Phys. Fluids*, **13**, pp. 3756-3774.
- [33] Tennekes, H. and Lumley, J. L., 1972 "A First Course in Turbulence," MIT Press.
- [34] Tsinober, A., 2000, "Vortex stretching versus production of strain/dissipation. *Turbulence Structure and Vortex Dynamics*," edited by Hunt, J. C. R. and Vassilicos, J. C., Cambridge University Press. 2000.
- [35] Kareem, W. A., Izawa, S., Xiong. A. K. and Fukunishi, Y., 2007, "Extraction and tracking of multi-scaled vortices from a homogeneous isotropic turbulent field," *J. Turbulence*, **8**, pp. 1-15.
- [36] Kareem, W. A., Izawa, S., Xiong. A. K. and Fukunishi, Y., 2006, "Identification of multi-scale coherent eddy structures in a homogeneous isotropic turbulence," *Progress in Computational Fluid Dynamics*, **6**, pp. 402-408.